Received: 2 June 2021 | Revised: 17 October 2021 | Accepted: 9 November 2021

DOI: 10.1002/psp4.12747

ARTICLE

A semimechanistic population pharmacokinetic and pharmacodynamic model incorporating autoinduction for the dose justification of TAS-114

Hikari Araki[1] | **Toru Takenaka**[1] | **Koichi Takahashi**[1] | **Fumiaki Yamashita**[1] | **Kazuaki Matsuoka**[1] | **Kunihiro Yoshisue**[1] | **Ichiro Ieiri**[2,3]

[1]Pharmacokinetics Research Laboratories, Taiho Pharmaceutical Co. Ltd., Tsukuba, Ibaraki, Japan

[2]Department of Clinical Pharmacology and Biopharmaceutics, Graduate School of Pharmaceutical Sciences, Kyushu University, Fukuoka, Japan

[3]Department of Pharmacy, Kyushu University Hospital, Fukuoka, Japan

Correspondence
Ichiro Ieiri, 3-1-1 Maidashi, Higashi-ku, Fukuoka 812-8582, Japan.
Email: ieiri@phar.kyushu-u.ac.jp

Funding information
All research activities were funded by Taiho Oncology, Inc., and Taiho Pharmaceutical Co., Ltd.

Abstract

TAS-114 is a dual deoxyuridine triphosphatase (dUTPase) and dihydropyrimidine dehydrogenase (DPD) inhibitor expected to widen the therapeutic index of capecitabine. Its maximum tolerated dose (MTD) was determined from a safety perspective in a combination study with capecitabine; however, its inhibitory effects on DPD activity were not assessed in the study. The dose justification to select its MTD as the recommended dose in terms of DPD inhibition has been required, but the autoinduction profile of TAS-114 made it difficult. To this end, an approach using a population pharmacokinetic (PPK)/pharmacodynamic (PD) model incorporating autoinduction was planned; however, the utility of this approach in the dose justification has not been reported. Thus, the aim of this study was to demonstrate the utility of a PPK/PD model incorporating autoinduction in the dose justification via a case study of TAS-114. Plasma concentrations of TAS-114 from 185 subjects and those of the endogenous DPD substrate uracil from 24 subjects were used. A two-compartment model with first-order absorption with lag time and an enzyme turnover model were selected for the pharmacokinetic (PK) model. Moreover, an indirect response model was selected for the PD model to capture the changes in plasma uracil concentrations. Model-based simulations provided the dose justification that DPD inhibition by TAS-114 reached a plateau level at the MTD, whereas exposures of TAS-114 increased dose dependently. Thus, the utility of a PPK/PD model incorporating autoinduction in the dose justification was demonstrated via this case study of TAS-114.

Study Highlights

WHAT IS THE CURRENT KNOWLEDGE ON THE TOPIC?

The maximum tolerated dose (MTD) of TAS-114 was determined in a clinical trial; however, its dihydropyrimidine dehydrogenase (DPD) inhibition at the MTD was not assessed. The dose justification of its MTD in terms of DPD inhibition was

required, but its autoinduction profile made it difficult. Moreover, the utility of a population pharmacokinetic (PPK)/pharmacodynamic (PD) model incorporating autoinduction in the dose justification has not been assessed.

WHAT QUESTION DID THIS STUDY ADDRESS?

This study provided the dose justification of its MTD by a PPK/PD model incorporating autoinduction. This study also demonstrated the utility of the model in the dose justification via a case study of TAS-114.

WHAT DOES THIS STUDY ADD TO OUR KNOWLEDGE?

A PPK/PD model incorporating autoinduction helps adjust and justify the clinical doses of drugs with autoinduction more appropriately.

HOW MIGHT THIS CHANGE DRUG DISCOVERY, DEVELOPMENT, AND/OR THERAPEUTICS?

TAS-114 could be integrated into a combination therapy with capecitabine. A PPK/PD model incorporating autoinduction can also help optimize clinical doses of other drugs with autoinduction.

INTRODUCTION

5-Fluorouracil (5-FU) has been used in various cancers for more than 50 years. The development of capecitabine, a prodrug of 5-FU, was an attempt to increase its efficacy.[1] However, high expression of the gatekeeper enzyme deoxyuridine triphosphatase (dUTPase), which prevents 5-FU from misincorporating into DNA, has been reported to be one of the mechanisms of acquired resistance.[2–5] In addition, patients treated with capecitabine experience toxicities, such as the hand–foot syndrome (HFS).[6,7] Although HFS is not a life-threatening toxicity, it adversely affects the patient's quality of life and results in dose reduction or interruption of capecitabine.[8,9] A retrospective analysis indicated that the catabolizing pathway of 5-FU could partly contribute to HFS occurrence, and inhibitors of dihydropyrimidine dehydrogenase (DPD), a rate-limiting enzyme of 5-FU degradation, could diminish the incidence of HFS.[8]

TAS-114 is a dual inhibitor of dUTPase and DPD[10–12] (Figure S1). Although TAS-114 does not have antitumor activity per se, it has the potential to widen the therapeutic index of capecitabine by lowering the dosage of capecitabine and HFS occurrence via DPD inhibition and enhancing antitumor efficacy via dUTPase inhibition.[11] To date, dUTPase inhibition by TAS-114 has not been directly observed in vivo as there was a lack of information on dUTPase activity. However, its effects on DPD activity were inferred from the changes in endogenous DPD substrate uracil concentrations in healthy male volunteers.[10] A safety perspective in a combination study on TAS-114 plus capecitabine established that the maximum tolerated dose (MTD) of TAS-114 was 360 mg/m^2, which corresponds to approximately 600 mg/body when calculated from the median body surface area (BSA) value: 1.70 m^2/body.[13] In contrast, the inhibitory effects of TAS-114 on DPD activity were not assessed in the study. Therefore, the dose justification to select its MTD as the recommended dose in terms of DPD inhibition is required.

In preclinical studies, it was shown that cytochrome P450 (CYP) 3A4 is the main enzyme responsible for TAS-114 metabolism, and TAS-114 can induce CYP3A.[10] In addition, the CYP3A induction profile of TAS-114 was observed in vivo by measuring the ratio of urinary concentration of 6β-hydroxycortisol (6β-OHF) to that of cortisol (F) on Days 0, 1, 7, 14, and 21 at 160 mg/m^2 or higher doses in a phase I study.[12] The ratio was used as an index of CYP3A activity in the study.[14,15] Moreover, the comparison of the area under the plasma concentration–time curve on Day 1 with those on the other days of the study indicated that induced CYP3A activities reduced systemic exposures of TAS-114.[12] These results indicated the autoinduction profile of TAS-114 in vivo; however, this profile made it difficult to estimate its systemic exposures and DPD inhibition to justify the MTD as the recommended dose of TAS-114.

The utility of a semimechanistic population pharmacokinetic (PPK) model incorporating autoinduction in the estimation of systemic exposures has been reported in several drugs with autoinduction profiles.[16–21] However, to the best of our knowledge, no prior study has attempted to expand the model into the estimation of pharmacodynamic (PD) responses. Moreover, the utility of a PPK/PD model incorporating autoinduction in clinical development, especially in the dose justification, has not been reported. Therefore, in the present study, our aim was to demonstrate the utility of a PPK/PD model incorporating autoinduction in the dose justification via a case study of TAS-114.

METHODS

Study design and subjects

Clinical and pharmacokinetic (PK) data of 185 subjects from 4 clinical trials, study 10057010 (clinical trial identifier: JapicCTI-111561), study 10057020 (NCT01610479), TPU-TAS-114-101 (NCT02025803), and TPU-TAS-114-102 (NCT02454062), were used for this study.[10,12,13,22] These trials were conducted in accordance with the Declaration of Helsinki and Good Clinical Practice guidelines and approved by the institutional review boards of the participating centers. All patients provided written informed consent. The subjects who were enrolled in the studies were healthy male subjects in Study 10057010, patients with histologically or cytologically confirmed solid tumors in whom the standard or other standard-equivalent therapy was ineffective or inappropriate in Study 10057020, patients with histologically or cytologically confirmed advanced solid tumors treated with standard anticancer therapy in Study TPU-TAS-114-101, and patients with histologically or cytologically confirmed advanced solid tumors and those who failed all standard therapies in Study TPU-TAS-114-102.

Drug administration, blood sampling, and bioanalysis

In Study 10057010, the subjects in the single-dose cohort were administered TAS-114 once, whereas those in the multiple-dose cohort received TAS-114 twice daily for 14 consecutive days and then once on Day 22.[10] In other studies, each subject was concurrently administered TAS-114 and S-1 or capecitabine twice daily for 14 consecutive days followed by a 7-day rest. This 21-day treatment cycle was maintained until disease progression, unacceptable toxicity, or withdrawal of consent. Numbers of subjects, dose ranges, cotreatments, and planned sampling designs and times are summarized in Table 1. Subject demographics are summarized in Table 2. Plasma TAS-114 and uracil concentrations were measured by validated bioanalytical methods using liquid chromatography/mass spectrometry at PK research laboratories of Taiho Pharmaceutical Co., Ltd., Tokyo, Japan, and at the PK and bioanalysis center of Shin Nippon Biomedical Laboratories, Ltd., Tokyo, Japan. The lower limit of quantification was 5 ng/ml for TAS-114 and 5 ng/ml for uracil, respectively.

TABLE 1 Clinical trial data used in population pharmacokinetic and pharmacodynamic analyses

Study number (clinical trial identifier)	No. of subjects	Range of TAS-114 dosage (mg)	Concomitant treatment	Dosing regimen	Planned sampling design	Planned sampling time
10057010 (JapicCTI-111561)	28	6–300	None	Once for single-dose cohort, twice daily for 14 consecutive days, and then once on day 22 for multiple-dose cohort	Days 1, 2, and 3 for single-dose cohort; Days 1, 3, 8, 14, and 22 for multiple-dose cohort	Predose, 0.5, 1, 2, 4, 6, 8, 12, 24, 48, and 72 h postdose for single-dose cohort; predose, 0.5, 1, 2, 4, 6, 8, and 12 h postdose for multiple-dose cohort
10057020 (NCT01610479)	68	6–480	S-1	Twice daily concurrently with S-1 for 14 consecutive days followed by a 7-day rest	Days 1, 7, 14, and 22	Predose, 1, 2, 4, 6, 8, and 12 h postdose
TPU-TAS-114-101 (NCT02025803)	41	14–800	Capecitabine	Twice daily concurrently with capecitabine for 14 consecutive days followed by a 7-day rest	Days 1 and 14	Predose, 0.5, 1, 2, 4, 6, and 8 h postdose
TPU-TAS-114-102 (NCT02454062)	48	9–600	S-1	Twice daily concurrently with S-1 for 14 consecutive days followed by a 7-day rest	Day 1	Predose, 1, 2, 4, 6, 8, and 12 h postdose

TABLE 2 Demographics of subjects in data set

Subject characteristics	Median (range) or number
Age (years)	59 (20–81)
Body weight (kg)	62 (36–119)
Height (cm)	166 (145–193)
Body surface area (m^2)	1.70 (1.25–2.35)
Sex (male/female)	106/79
Race (Japanese/Caucasian/African American/others)	96/77/7/5
ALT (U/L)	19.0 (6.0–151.0)
AST (U/L)	24.0 (7.0–140.0)
BUN (mg/dl)	16.0 (5.7–354.2)

Abbreviations: ALT, alanine transaminase level (normal range, 4–36 U/L); AST, aspartate aminotransferase level (normal range, 8–33 U/L); BUN, blood urea nitrogen (normal range, 12–20 mg/dl).

PPK model development

A population PPK analysis was performed using NONMEM 7.3.0 (Icon Development Solutions) with first-order conditional estimation with interaction method. Perl-speaks-NONMEM (Version 4.8.1) was used in model development.[23,24] The NONMEM output was plotted with Xpose4 package (Version 4.6.1) developed for R (Version 3.6.3).[25,26] The values below the lower limit of quantification and plasma TAS-114 concentrations collected before administrations were not used in the modeling. For the base structure model, single-compartment and multiple-compartment models were tested to describe plasma TAS-114 concentration profiles. To depict the delay of absorption, lag time and transit absorption models were tested. The enzyme turnover model reported by Hassan et al.[16] was applied to characterize the temporal changes in enzyme amounts in an enzyme pool, which were expressed as follows:

$$\frac{dA_{enz,amount}}{dt} = k_{enz,in} \cdot \left[1 + f(C_p)\right] - k_{enz,deg} \cdot A_{enz,amount}$$

where $A_{enz,amount}$ is the amount of enzyme in the pool, $k_{enz,in}$ is the zero-order enzyme formation rate constant and $k_{enz,deg}$ is the first-order enzyme degradation rate constant, and $f(C_p)$ is the relationship between the concentrations in the central compartment and the enzyme formation rate. At time zero, $A_{enz,amout}$ is represented as its baseline $A_{enz,baseline}$, $f(C_p)$ is zero, and $k_{enz,in}$ is equal to $k_{enz,deg} \cdot A_{enz,baseline}$. Using the relative amount to baseline of the enzyme (A_{enz}), which is calculated by dividing the $A_{enz,amount}$ by $A_{enz,baseline}$, the above equation could be rewritten as follows:

$$\frac{dA_{enz}}{dt} = k_{enz,deg} \cdot \left[1 + f(C_p)\right] - k_{enz,deg} \cdot A_{enz}$$

As an enzyme induction can be expressed by the maximum induction effect (E_{max}) model, we used the E_{max} model as a nonlinear function for the $f(C_p)$. However, in cases in which plasma TAS-114 concentrations are much less than the values at concentration at the half maximum induction (EC_{50}), the aforementioned E_{max} model can be rewritten as the linear function using SLOPE, which represents the ratio of E_{max}/EC_{50}. Thus, we tested the following equations as $f(C_p)$:

$$f(C_p) = \text{SLOPE} \cdot C_p$$

$$f\left(C_p\right) = \frac{E_{max} \cdot C_p}{EC_{50} + C_p}$$

where SLOPE is the apparent constant that represents the ratio of E_{max}/EC_{50}.

Exponential and proportional error models were selected to describe the interindividual variability (IIV) and residual variability, respectively. Covariate modeling was conducted after the basic model development. Subjects' information, such as sex, BSA, age, aspartate aminotransferase level (AST), and blood urea nitrogen, was tested as covariates. Covariates were selected according to their biological plausibility and reductions of the object function values (OFVs) estimated by NONMEM after they were incorporated in the model following forward inclusion and backward exclusion procedures. Forward inclusion and backward exclusion were applied for the development of covariate models. Significance levels for forward inclusion and backward exclusion were set at 0.01 and 0.001, respectively. Effects of continuous covariates on PK parameters were parameterized by exponential and power functions, respectively, as the following:

$$P_i = tvP \cdot e^{\theta_{cov} \cdot (COV - COV_{median})}$$

$$P_i = tvP \cdot \left(\frac{COV}{COV_{median}}\right)^{\theta_{COV}}$$

where P_i is the individual value of a parameter, tvP is the typical value of a parameter, θ_{COV} is the fractional change in a parameter, COV is the individual value of a covariate, and COV_{median} is the median value of a covariate.

Effects of categorical covariates were parameterized by a linear function as:

$$P_i = tvP \cdot \left(1 + \theta_{COV} \cdot COV\right)$$

where P_i is the individual value of a parameter, tvP is the typical value of a parameter, θ_{COV} is the fractional change

in a parameter, and COV is the individual value of a covariate.

PPK/PD model development

As DPD converts its endogenous substrate uracil to dihydrouracil, plasma uracil concentrations after TAS-114 administration were collected in Study 10057010 and used for the PPK/PD modeling.[10] There was a time discrepancy in the relationship between plasma TAS-114 concentrations and observed uracil concentrations. In addition, the time to peak effects was delayed by dose increases. Thus, changes in observed plasma uracil concentrations were modeled using an indirect response model.[27,28] For the PD model development, we assumed that uracil was eliminated by an irreversible metabolic process in the liver, and urinary excretion of uracil was ignored because reported urinary excretion percentages of uracil were from 0.7% to 2.3% of doses.[29] A sequential method with modal posterior Bayes estimates of the individual PK parameters was applied to build the model.[30] The first-order rate constant for the elimination of uracil (k_{out}) was calculated using the reported half-life ($T_{1/2}$) value after oral administration of 50 mg uracil and incorporated in the model.[29] The baseline of plasma uracil concentrations was handled by incorporating IIV into it.[31] Exponential and proportional error models were selected to describe the IIV and residual variability, respectively. Covariate modeling was conducted after the basic model development.

Model selection

Models were evaluated by changes in OFV, Akaike information criterion, relative standard errors, condition numbers that should be lower than 1000, and goodness-of-fit (GOF) plots that were plots of the observation versus population prediction (PRED) and individual predictions (IPRED), conditional weighted residuals (CWRES) versus the treatment duration, CWRES versus PRED, and absolute individual weighted residuals versus IPRED. To assess the predictability of TAS-114 and uracil concentrations by the final model, a prediction-corrected visual predictive check (pcVPC) was conducted by 1000 simulations.[32] A 90% prediction interval was defined for pcVPC from the 5th and 95th percentiles of simulated dependent data at each timepoint and was then compared with original data. The robustness of the final model was assessed by the bootstrap method with 1000 resamplings from original data sets. Final estimates from original data sets were compared with the median and 95% lower and upper limits of the confidence interval calculated from the bootstrap.

Model-based simulation

To estimate the median of TAS-114 systemic exposures and its DPD inhibition at various doses, we simulated the time course changes in the oral clearance (CL/F) and PK of TAS-114 and plasma uracil concentrations using the developed model. A relative CL/F of TAS-114 to the baseline value of CL/F and plasma TAS-114 and uracil concentrations were simulated for 1000 replicates at each timepoint after repeated TAS-114 administrations of doses from 6 to 800 mg/body twice daily for 14 consecutive days. The time course of relative CL/F over 14 days was plotted against the number of days after the first TAS-114 administration. The median of area under the plasma concentration–time curve from the time 0 to the time of the last measurable plasma concentration (AUC_{last}), maximum observed plasma concentration (C_{max}), and minimum and maximum inhibitory percentages of TAS-114-mediated uracil metabolism at the steady state (Days 14 to 14.5) were plotted against doses.

RESULTS

Data

A total of 2661 points of plasma TAS-114 concentrations obtained from 185 subjects, and 240 points of plasma uracil concentrations obtained from 24 healthy male volunteers were used in the model development. Subjects were administered from 6 to 800 mg/body (median, 270 mg/body) of TAS-114. Subject demographics are summarized in Table 2. Median age, BSA, and AST, which were finally selected as covariates, were 59 years (range, 20–81 years), 1.70 m^2 (range, 1.25–2.35 m^2), and 24 U/L (range, 7–140 U/L), respectively.

PPK model

An overview of the PPK/PD model of TAS-114 is shown in Figure 1, and final estimates of the PK parameters are shown in Table 3.

A two-compartment model incorporating an enzyme turnover model with first-order absorption with lag time was selected as the base structure of the PPK model of TAS-114. In the enzyme turnover model, the stimulation process of enzyme production was described by the E_{max} model with a nonlinear relationship between TAS-114 concentration in the central compartment and the

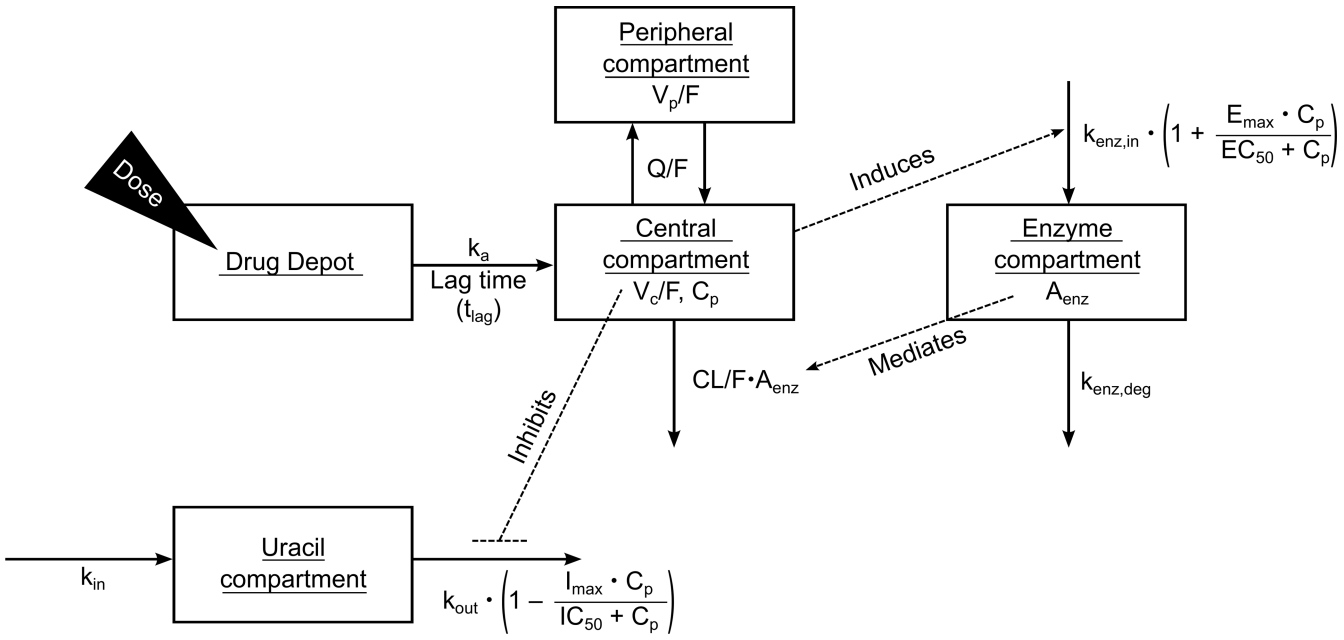

FIGURE 1 Schematic representation of the population pharmacokinetic and pharmacodynamic model of TAS-114. A_{enz}, relative amount to the baseline of enzyme; CL/F, oral clearance; C_p, concentration in the central compartment; EC_{50}; concentration at half maximum induction; E_{max}, maximum induction effect; IC_{50}, concentration at half maximum inhibition; I_{max}, maximum inhibitory effect; k_a, absorption rate constant; $k_{enz,in}$, zero-order enzyme formation rate constant; $k_{enz,deg}$, first-order enzyme degradation rate constant; k_{in}, zero-order rate constant for production of uracil; k_{out}, first-order rate constant for the elimination of uracil; Q/F, intercompartmental clearance; t_{lag}, absorption lag time; V_c/F, distribution volume of the central compartment; V_p/F, distribution volume of the peripheral compartment

enzyme formation rate constant. The parameter E_{max} and EC_{50} in the E_{max} model were estimated to be 4.69 and 5870 (ng/ml), respectively. The $k_{enz,deg}$ and the corresponding $T_{1/2}$ were estimated to be 0.0230 (h^{-1}) and 30.1 (h), respectively. These estimates indicate that it takes approximately 6 days to return from the induced state by TAS-114 to the baseline. The effects of changes in relative amounts of enzyme on CL/F of TAS-114 were described by a linear relationship.

Age and AST on CL/F and BSA on distribution volume of the central compartment (V_c/F) were selected as covariates. Ratios of the PK parameter with the first-quartile covariate value to those with the third-quartile covariate value were 1.4 for age on CL/F, 1.1 for AST on CL/F, and 0.7 for BSA on V_c/F, respectively. Thus, the influences of these covariates on the parameters were limited.

The final model was verified by the GOF plot in Figure S2, pcVPC plots stratified by sampling days in Figure 2a–d, VPC plots stratified by TAS-114 dosage in Figure S3, and the 1000 bootstrap replicates in Table 3. The bootstrap convergence rate was 90.8% in 1000 replicates.

PPK/PD model

An overview of the PPK/PD model of TAS-114 is shown in Figure 1, and final estimates of the PD parameters are shown in Table 4.

An indirect response model was selected as the base structure to capture the time course changes in plasma uracil concentrations. The parameter k_{out} was fixed at 2.67 (h^{-1}) corresponding to 0.260 (h) as $T_{1/2}$. These values imply that it takes approximately 1.3 (h) to return from the inhibited state by TAS-114 to the baseline. The concentration at half maximum inhibition (IC_{50}) and maximum inhibitory effect were estimated to be 1046 (ng/ml) and 0.888, respectively. The baseline of plasma uracil concentration (Baseline) was estimated to be 9.27 (ng/ml). No subject information was selected as covariates.

The final model was verified by the GOF plot in Figure S5, pcVPC in Figure 2e, and the 1000 bootstrap replicates in Table 4. The bootstrap convergence rate was 99.6% in 1000 replicates.

Simulation

We applied the developed model to simulate the time course changes in the CL/F and PK of TAS-114 and the changes in plasma uracil concentrations. Simulated values of the relative CL/F of TAS-114 to the baseline values, AUC_{last} and C_{max} of TAS-114, and maximum and minimum inhibition percentages of TAS-114-mediated uracil metabolism were summarized in

TABLE 3 Parameter estimates and bootstrap results for the final population pharmacokinetic model

Parameter	Original data set			1000 Bootstrap replicates			Bootstrap/final estimate ratio
	Estimate	RSE (%)	Shrinkage (%)	Median	95% LLCI	95% ULCI	
Population mean							
k_a (h^{-1})	0.508	3.6	N/A	0.504	0.439	0.611	0.99
V_c/F (L)	17.0	7.0	N/A	17.1	12.5	22.8	1.00
V_p/F (L)	10.5	5.7	N/A	10.4	8.8	13.1	0.99
Q/F (L/h)	4.02	13.1	N/A	3.97	1.77	5.72	0.99
CL/F (L/h)	8.74	6.2	N/A	8.73	7.77	9.66	1.00
E_{max}	4.69	24.0	N/A	4.72	2.50	13.76	1.01
EC_{50} (ng/ml)	5870	28.2	N/A	5849	1949	26,147	1.00
$k_{enz,deg}$ (h^{-1})	0.0230	16.4	N/A	0.0230	0.0198	0.0266	1.00
t_{lag} (h)	0.217	8.4	N/A	0.219	0.122	0.299	1.01
Effects of BSA on V_c/F	1.52	21.4	N/A	1.51	1.07	1.99	1.00
Effects of AST on CL/F	−0.00753	19.2	N/A	−0.00741	−0.01304	−0.00185	0.98
Effects of AGE on CL/F	−0.983	15.6	N/A	−0.988	−1.176	−0.786	1.00
IIV variability							
IIV k_a (CV%)	21.0	18.6	47.5	20.9	9.6	40.0	1.00
IIV V_c/F (CV%)	69.8	7.3	16.9	69.7	45.4	91.9	1.00
IIV CL/F (CV%)	65.7	5.3	2.3	64.6	55.5	74.9	0.98
Residual variability							
Proportional error (CV%)	61.0	0.6	3.0	60.8	59.0	62.7	1.00

Note: Bootstrap convergence rate 90.8% (908 successes and 92 failures in 1000 replicates). Bootstrap/final estimate ratios were calculated by dividing median values obtained from the bootstrap by final estimates from the original data set.

Abbreviations: AGE, age; AST, aspartate aminotransferase; BSA, body surface area; CL/F; oral clearance; CV, coefficient of variation; EC_{50}; concentration at half maximum induction; E_{max}; maximum induction effect, IIV, interindividual variability; 95% LLCI, lower limit of the 95% confidence interval; k_a, absorption rate constant; $k_{enz,deg}$, first-order enzyme degradation rate constant; N/A, not applicable; Q/F, intercompartmental clearance; RSE, relative standard error; t_{lag}, absorption lag time; 95% ULCI, upper limit of the 95% confidence interval; V_c/F, distribution volume of the central compartment; V_p/F, distribution volume of the peripheral compartment.

Table S1. Relative CL/Fs of TAS-114 to the baseline value of CL/F were plotted against the number of days after the first administration in Figure 3a. The relative CL/F increased in a dose-dependent manner and a time-dependent manner during the dosing period. AUC_{last} and C_{max} were plotted against doses after a recurring 14-day TAS-114 administration in Figure 3b. Hence, AUC_{last} and C_{max} increased in a dose-dependent manner up to 800 mg/body despite dose-dependent increases in CL/F. In contrast, although inhibitory percentages of TAS-114-mediated uracil metabolism had high variability, the median of minimum and maximum inhibitory percentages of TAS-114-mediated uracil metabolism after the repeated 14-day TAS-114 administration cycle reached a plateau level at the MTD (600 mg/body) in Figure 3c.

DISCUSSION

In this study, we examined the utility of a PPK/PD model incorporating autoinduction in the dose justification via a case study of TAS-114. To this end, we developed a semi-mechanistic TAS-114 PPK/PD model incorporating autoinduction. Time-dependent changes in PK of TAS-114 were characterized by incorporating an enzyme turnover model into a base model. Moreover, we captured changes in plasma concentrations of uracil as an index of DPD activity by incorporating an indirect response model into a PPK model.

Dose-dependent effects on exposures of TAS-114 were evaluated in Study 10057020.[12] Exposures of TAS-114 increased dose dependently on Day 1, and the dose-dependent increases in exposures diminished on Day 7 and Day 14. Thus, we assumed that this time-dependent

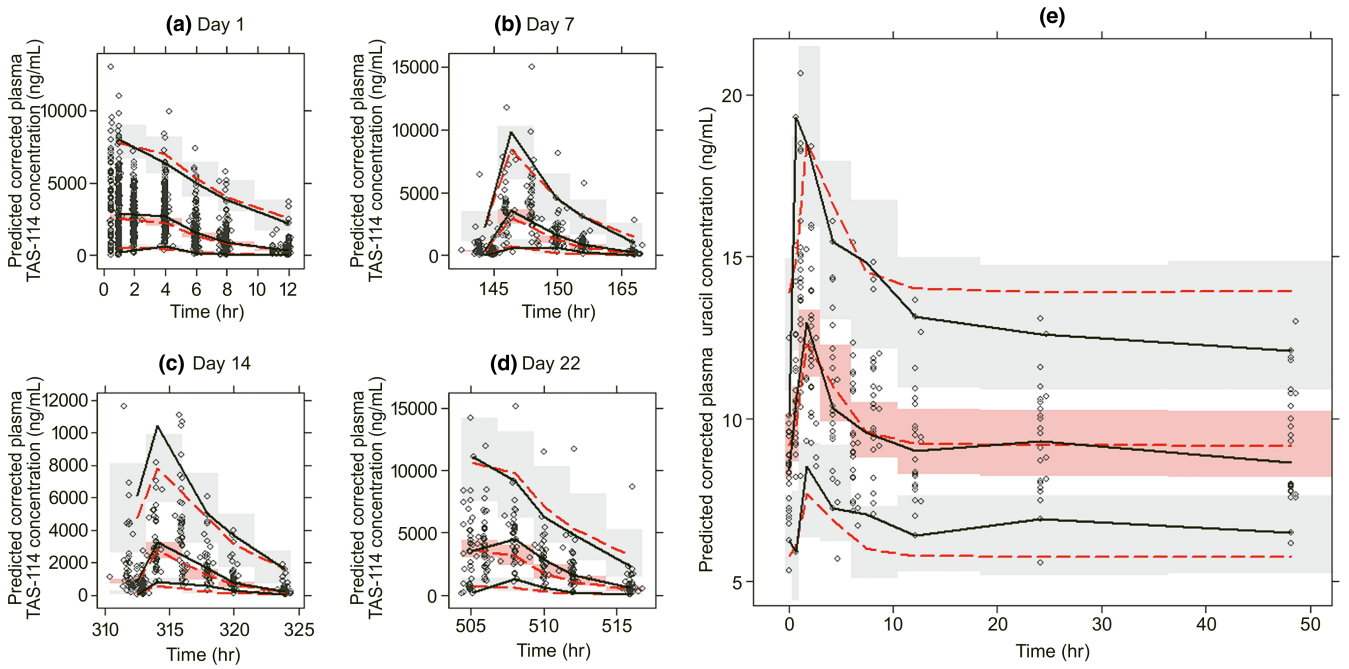

FIGURE 2 Prediction-corrected visual predictive check plots of plasma TAS-114 concentrations on (a) Day 1, (b) Day 7, (c) Day 14, and (d) Day 22, and (e) plasma uracil concentrations. Open circles represent prediction corrected observations. Black solid lines and red dashed lines represent the 5%, median, and 95% values of prediction-corrected observed and simulated data, respectively. Red areas represent the 95% confidence intervals on the simulated median. Gray areas represent the 95% confidence intervals on the simulated 5% and 95% values

TABLE 4 Parameter estimates and bootstrap results for the final population pharmacodynamic model

	Original data set			1000 Bootstrap replicates			
Parameter	**Estimate**	**RSE (%)**	**Shrinkage (%)**	**Median**	**95% LLCI**	**95% ULCI**	**Bootstrap/final estimate ratio**
Population mean							
k_{out} (h^{-1})	2.67	Fixed	N/A	2.67	Fixed	Fixed	N/A
IC_{50} (ng/ml)	1046	21.7	N/A	1057	772	1473	1.01
I_{max}	0.888	8.5	N/A	0.891	0.794	1.000	1.00
Baseline (ng/ml)	9.27	3.5	N/A	9.28	8.65	9.93	1.00
IIV variability							
IIV baseline (CV%)	15.4	15.4	2.7	15.0	9.5	20.0	0.98
Residual variability							
Proportional error (CV%)	39.9	1.4	4.4	39.8	36.4	42.4	1.00

Note: Bootstrap convergence rate 99.6% (996 successes and 4 failures in 1000 replicates). Bootstrap/final estimate ratios were calculated by dividing median values obtained from the bootstrap by final estimates from the original data set.

Abbreviations: Baseline; baseline of plasma uracil concentration; CV, coefficient of variation; IC_{50}, concentration at half maximum inhibition; IIV, interindividual variability; I_{max}, maximum inhibitory effect; k_{out}, first-order rate constant for the elimination of uracil; 95% LLCI, lower limit of the 95% confidence interval; N/A, not applicable; RSE, relative standard error; 95% ULCI, upper limit of the 95% confidence interval.

decreases in exposures could be explained by the autoinduction rather than dose-dependent effects. We modeled the mechanism by which TAS-114 stimulates the synthesis rate of CYP3A that metabolizes TAS-114 via an enzyme turnover model to describe the time course of plasma TAS-114 concentrations. Modeling the stimulation process of the enzyme synthesis rate was also applied to other drugs with autoinduction profiles, such as cyclophosphamide,[16] rifampicin,[19,20] and mitotane.[21] Based on the final model, the $k_{enz,deg}$, and its corresponding $T_{1/2}$ were estimated to be 0.0230 (h^{-1}) and 30.1 (h), respectively. The in vitro degradation rate constants of hepatic CYP3A (k_{deg}) and its corresponding $T_{1/2}$ ranged from 0.0138 to 0.0240 (h^{-1}) for k_{deg} and from 29.0 to 51.4 (h) for $T_{1/2}$, respectively.[33–35] In prior

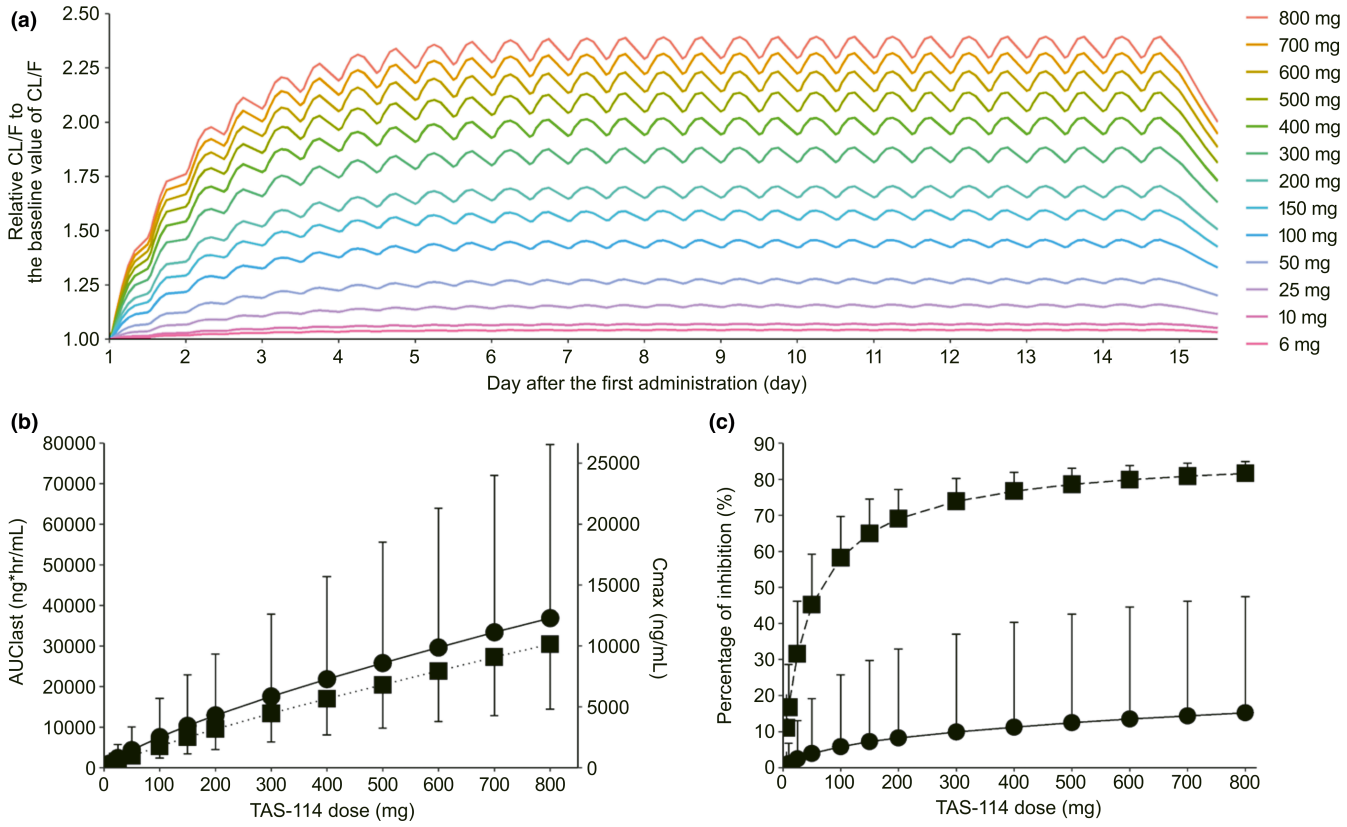

FIGURE 3 Simulated relative CL/F of TAS-114 to the baseline value of CL/F after multiple TAS-114 administrations for (a) 14 days, (b) AUC_{last} and C_{max} of TAS-114, and (c) maximum and minimum inhibition percentages of TAS-114-mediated uracil metabolism on Day 14. (a) Each solid line represents the median relative CL/F of TAS-114 to the baseline value of CL/F after multiple TAS-114 administrations. From the bottom to the top of the figure, relative CL/Fs at 6, 10, 25, 50, 100, 150, 200, 300, 400, 500, 600, 700, and 800 mg/body of TAS-114 are plotted. (b) Closed circles and closed squares represent AUC_{last} and C_{max}, respectively, from 6 to 800 mg of TAS-114 on Day 14. Each point is the median of simulations. Each error bar represents the 95% prediction interval. (c) Closed circles and closed squares represent minimum and maximum inhibition percentages, respectively, of TAS-114-mediated uracil metabolism on Day 14. Each point is the median value of simulations. Each error bar represents the 95% prediction interval. AUC_{last}, area under the plasma concentration–time curve from the time 0 to the time of the last measurable plasma concentration; CL/F, oral clearance; C_{max}, maximum observed plasma concentration

clinical trials, $T_{1/2}$ of CYP3A was ranged from 10.0 to 140 (h).[36–38] The $k_{enz,deg}$ and its corresponding $T_{1/2}$ estimated from the final model were all within the range of reported values. Then, we compared the simulated time course of relative CL/F with the observed in vivo urinary 6β-OHF/F ratios to verify the estimated induction parameters. The relative CL/Fs from 200 mg/body to 400 mg/body at the steady state were simulated to be approximately 1.7 to 2.0 as shown in Figure 3a. The maximum degrees were approximately 1.7 to 2.0 for the urinary 6β-OHF/F ratios observed in a phase I study from Day 1 to Day 14 at over 160 mg/m^2 (270–400 mg/body).[12] As the simulated relative CL/Fs were consistent with the observed in vivo urinary 6β-OHF/F ratios, the induction parameters were reasonably estimated. IIVs are useful for estimating individual systemic exposures of TAS-114. However, IIVs on induction parameters could not be calculated here as vital information was missing, such as plasma concentrations before reaching the steady state of induction and during a 1-week cessation of TAS-114 when the induced enzyme returned to the baseline.

In the PPK/PD modeling, inhibitory effects of TAS-114 on DPD activity were modeled using changes in the plasma concentrations of endogenous DPD substrate uracil. An indirect response model was selected to capture the time course of plasma uracil concentrations because of delays in PD responses to plasma TAS-114 concentrations and dose-dependent delays in the peak effect time.[27,28,39] As plasma dihydrouracil concentrations after TAS-114 administration were also collected in Study 10057010, we tested indirect response models reflecting the changes in plasma dihydrouracil concentrations or the plasma dihydrouracil/uracil concentration ratios. The latter is reported as a surrogate DPD activity marker.[40,41] We also tested a precursor-dependent indirect PD response model using plasma uracil and dihydrouracil concentrations.[42] Nevertheless, none of the foregoing models improved the fit. Especially, a precursor model should have more

flexibility than other models; however, it needed more data to estimate increased parameters. In this study, limited information obtained from 24 subjects made it difficult to estimate increased parameters and run the model stably. It was recently discovered that the plasma uracil concentration is more strongly correlated with DPD activity in peripheral blood mononuclear cells than the plasma dihydrouracil/uracil concentration ratio.[43] Therefore, we used the plasma uracil concentration for the modeling. Plasma uracil concentrations were collected at the same blood sampling time, under 10 h of fasting before administration and 4 h of fasting after administration and with the same meals for all patients. Therefore, the influences of the circadian rhythm of DPD activity and the impact of ingesta containing uracil or its precursor uridine on plasma uracil concentrations can be excluded from the model.[9,41,44] The estimated IC_{50} was 1046 (ng/ml). The k_i value of TAS-114 was 966 (ng/ml); it was obtained by evaluating the inhibitory effects of TAS-114 on DPD-mediated 5-FU metabolism in the human liver S9 fractions.[11] Therefore, the IC_{50} estimated by this model was deemed reasonable. Abundant predose samples enabled estimation of the median and IIV of the baseline of plasma uracil concentrations. The estimates were consistent with the reported medians.[45] However, IIVs of other parameters could not be estimated because of insufficient information. Therefore, more data should be collected in the subsequent phases to estimate IIVs for the other parameters.

In a 3 + 3 study design combining TAS-114 and capecitabine, the TAS-114 MTD was determined to be 600 mg/body under the condition of twice daily for 14 consecutive days.[13] We tried to justify its MTD as the recommended dose in terms of DPD inhibition via simulations at various dosages using the developed model. The simulated relative CL/Fs increased in a dose-dependent manner and a time-dependent manner because of autoinduction. TAS-114 exposures increased in a dose-dependent manner up to 800 mg/body. However, the median of minimum and maximum inhibitory percentages of TAS-114-mediated uracil metabolism reached a plateau level at the MTD (600 mg/body). The model-based simulations provided the dose justification that the predetermined TAS-114 MTD (600 mg/body) sufficed to inhibit DPD activity under the condition of twice daily for 14 consecutive days. From a different point of view, the dose reduction of TAS-114 could be proposed by simulated results. TAS-114 was designed as a dual inhibitor of dUTPase and DPD, and TAS-114 was expected to enhance the antitumor efficacy of 5-FU via its dUTPase inhibition.[10-13,22,46–48] However, the inhibitory effects of TAS-114 on dUTPase activity were not modeled in this study because the information for dUTPase activity was not collected in past clinical studies. Therefore, it was not enough to propose the dose reduction of TAS-114 only in terms of its DPD inhibition. Future research should assess the additional inhibitory effects of TAS-114 on dUTPase activity by collecting the surrogate biomarker information for dUTPase activity in further clinical trials to adjust TAS-114 dosages. Moreover, to evaluate the influences of TAS-114-mediated DPD inhibition on exposures, efficacies, and toxicities such as HFS of capecitabine, this model needs to be combined with the PPK/PD model of capecitabine. To establish the PPK/PD model of capecitabine considering inhibitory effects of TAS-114 on DPD activity, the information including plasma concentrations of capecitabine and its metabolites, response evaluations in solid tumors, and the incidences of HFS are needed from further clinical trials. Constructing this combined model will enable us to adjust both TAS-114 and capecitabine dosages considering the influence of TAS-114 on antitumor efficacy and toxicity of capecitabine. Furthermore, the correlation between the DPD activity and the incidence of HFS by capecitabine has not been quantified until now. This model can also be applied to quantify it and will enable us to optimize the target subject number in future clinical trials.

The dose adjustment and justification are keys for success in overall drug development. A PPK/PD model enables us to understand the relationship between concentrations and PD responses. It also allows us to adjust and justify the clinical dosage by identifying subjects' information and quantifying the magnitude of the unexplained variability that alters exposures and PD responses. Moreover, the PPK/PD model incorporating autoinduction shown here provides us information, including the time course and magnitude of changes in metabolic enzyme expressions that influence exposures and PD responses of each drug with autoinduction. Therefore, it is useful to adjust and justify the clinical dosage more appropriately in case of clinical development of drugs with autoinduction.

In this study, we successfully developed a semimechanistic TAS-114 PPK/PD model incorporating autoinduction. The model-based simulations provided the dose justification of the TAS-114 MTD for DPD inhibition under the condition of twice daily for 14 consecutive days. Moreover, the utility of this model in the dose justification was demonstrated via the case study of TAS-114. We expect that TAS-114 combined with capecitabine will comprise a new novel 5-FU combination therapy. Furthermore, the PPK/PD model incorporating autoinduction can be applied in the clinical development of other drugs with autoinduction profiles and help optimize their dosages.

ACKNOWLEDGMENTS

We thank all of the participating subjects in the clinical studies, the study investigators, study nurses, study

monitors, data managers, and all team members of TAS-114. We also thank Editage for English-language editing services.

CONFLICT OF INTEREST

H.A., T.T., K.T., F.Y., K.M., and K.Y. are employees of Taiho Pharmaceutical Co., Ltd. I.I. has declared no competing interests for this work.

AUTHOR CONTRIBUTIONS

H.A., T.T., K.T., and F.Y. designed and performed the research and analyzed the data. H.A., K.M., K.Y., and I.I. wrote the manuscript. K.M., K.Y., and I.I. designed the research.

ORCID

Hikari Araki https://orcid.org/0000-0002-0254-9975

REFERENCES

1. Di Costanzo F, Sdrobolini A, Gasperoni S. Capecitabine, a new oral fluoropyrimidine for the treatment of colorectal cancer. *Crit Rev Oncol*. 2000;35:101-108.
2. Ladner RD, Lynch FJ, Groshen S, et al. dUTP nucleotidohydrolase isoform expression in normal and neoplastic tissues: association with survival and response to 5-fluorouracil in colorectal cancer. *Cancer Res*. 2000;60:3493-3503.
3. Kawahara A, Akagi Y, Hattori S, et al. Higher expression of deoxyuridine triphosphatase (dUTPase) may predict the metastasis potential of colorectal cancer. *J Clin Pathol*. 2009;62:364-369.
4. Takatori H, Yamashita T, Honda M, et al. dUTP pyrophosphatase expression correlates with a poor prognosis in hepatocellular carcinoma. *Liver Int*. 2010;30:438-446.
5. Wilson PM, Fazzone W, LaBonte MJ, Deng J, Neamati N, Ladner RD. Novel opportunities for thymidylate metabolism as a therapeutic target. *Mol Cancer Ther*. 2008;7:3029-3037.
6. Saif MW, Choma A, Salamone SJ, Chu E. Pharmacokinetically guided dose adjustment of 5-fluorouracil: a rational approach to improving therapeutic outcomes. *J Natl Cancer Inst*. 2009;101:1543-1552.
7. Saif MW. Capecitabine and hand-foot syndrome. *Expert Opin Drug Saf*. 2011;10:159-169.
8. Yen-Revollo JL, Goldberg RM, McLeod HL. Can inhibiting dihydropyrimidine dehydrogenase limit hand-foot syndrome caused by fluoropyrimidines? *Clin Cancer Res*. 2008;14:8-13.
9. Jacobs BAW, Deenen MJ, Pluim D, et al. Pronounced between-subject and circadian variability in thymidylate synthase and dihydropyrimidine dehydrogenase enzyme activity in human volunteers. *Br J Clin Pharmacol*. 2016;82:706-716.
10. Saito K, Nagashima H, Noguchi K, et al. First-in-human, phase I dose-escalation study of single and multiple doses of a first-in-class enhancer of fluoropyrimidines, a dUTPase inhibitor (TAS-114) in healthy male volunteers. *Cancer Chemother Pharmacol*. 2014;73:577-583.
11. Yano W, Yokogawa T, Wakasa T, et al. TAS-114, a first-in-class dual dUTPase/DPD inhibitor, demonstrates potential to improve therapeutic efficacy of fluoropyrimidine-based chemotherapy. *Mol Cancer Ther*. 2018;17:1683-1693.
12. Doi T, Yoh K, Shitara K, et al. First-in-human phase 1 study of novel dUTPase inhibitor TAS-114 in combination with S-1 in Japanese patients with advanced solid tumors. *Invest New Drugs*. 2019;37(3):507-518.
13. LoRusso PM, et al. Abstract CT012: Phase I study of TAS-114 in combination with capecitabine in patients with advanced solid tumors. *Can Res*. 2018;78:CT012.
14. Shin KH, Choi MH, Lim KS, Yu KS, Jang IJ, Cho JY. Evaluation of endogenous metabolic markers of hepatic CYP3A activity using metabolic profiling and midazolam clearance. *Clin Pharmacol Ther*. 2013;94:601-609.
15. Shin KH, Ahn LY, Choi MH, et al. Urinary 6beta-hydroxycortisol/cortisol ratio most highly correlates with midazolam clearance under hepatic CYP3A inhibition and induction in females: a pharmacometabolomics approach. *AAPS J*. 2016;18:1254-1261.
16. Hassan, Svensson, Ljungman, et al. A mechanism-based pharmacokinetic-enzyme model for cyclophosphamide autoinduction in breast cancer patients. *Br J Clin Pharmacol*. 1999;48:669-677.
17. Kerbusch T, Huitema ADR, Ouwerkerk J, et al. Evaluation of the autoinduction of ifosfamide metabolism by a population pharmacokinetic approach using NONMEM. *Br J Clin Pharmacol*. 2000;49:555-561.
18. Yin OQP, Wang Y, Schran H. A mechanism-based population pharmacokinetic model for characterizing time-dependent pharmacokinetics of midostaurin and its metabolites in human subjects. *Clin Pharmacokinet*. 2008;47:807-816.
19. Smythe W, Khandelwal A, Merle C, et al. A semimechanistic pharmacokinetic-enzyme turnover model for rifampin autoinduction in adult tuberculosis patients. *Antimicrob Agents Chemother*. 2012;56:2091-2098.
20. Svensson RJ, Aarnoutse RE, Diacon AH, et al. A population pharmacokinetic model incorporating saturable pharmacokinetics and autoinduction for high rifampicin doses. *Clin Pharmacol Ther*. 2018;103:674-683.
21. Arshad U, Taubert M, Kurlbaum M, et al. Enzyme autoinduction by mitotane supported by population pharmacokinetic modelling in a large cohort of adrenocortical carcinoma patients. *Eur J Endocrinol*. 2018;179:287-297.
22. Fasolo A, Aoyama T, Stathis A, et al. Abstract CT014: a large phase I study of TAS-114 in combination with S-1 in patients with advanced solid tumors. *Cancer Res*. 2018;78:CT014.
23. Lindbom L, Ribbing J, Jonsson EN. Perl-speaks-NONMEM (PsN)–a Perl module for NONMEM related programming. *Comput Methods Programs Biomed*. 2004;75:85-94.
24. Lindbom L, Pihlgren P, Jonsson EN. PsN-Toolkit–a collection of computer intensive statistical methods for non-linear mixed effect modeling using NONMEM. *Comput Methods Programs Biomed*. 2005;79:241-257.
25. R Core Team. *R: A language and environment for statistical computing*. R Foundation for Statistical Computing. https://www.R-project.org/. Accessed March 16, 2021
26. Jonsson EN, Karlsson MO. Xpose—an S-PLUS based population pharmacokinetic/pharmacodynamic model building aid for NONMEM. *Comput Methods Programs Biomed*. 1998;58:51-64.
27. Dayneka NL, Garg V, Jusko WJ. Comparison of four basic models of indirect pharmacodynamic responses. *J Pharmacokinet Biopharm*. 1993;21:457-478.

28. Sharma A, Jusko WJ. Characterization of four basic models of indirect pharmacodynamic responses. *J Pharmacokinet Biopharm*. 1996;24:611-635.
29. Ito S, Kawamura T, Inada M, et al. Physiologically based pharmacokinetic modelling of the three-step metabolism of pyrimidine using C-uracil as an in vivo probe. *Br J Clin Pharmacol*. 2005;60:584-593.
30. Zhang L, Beal SL, Sheiner LB. Simultaneous vs. sequential analysis for population PK/PD data I: best-case performance. *J Pharmacokinet Pharmacodyn*. 2003;30:387-404.
31. Dansirikul C, Silber HE, Karlsson MO. Approaches to handling pharmacodynamic baseline responses. *J Pharmacokinet Pharmacodyn*. 2008;35:269-283.
32. Bergstrand M, Hooker AC, Wallin JE, Karlsson MO. Prediction-corrected visual predictive checks for diagnosing nonlinear mixed-effects models. *AAPS J*. 2011;13:143-151.
33. Ramsden D, Zhou J, Tweedie DJ. Determination of a degradation constant for CYP3A4 by direct suppression of mRNA in a novel human hepatocyte model, HepatoPac. *Drug Metab Dispos*. 2015;43:1307-1315.
34. Chan CYS, Roberts O, Rajoli RKR, et al. Derivation of CYP3A4 and CYP2B6 degradation rate constants in primary human hepatocytes: a siRNA-silencing-based approach. *Drug Metab Pharmacokinet*. 2018;33:179-187.
35. Obach RS, Walsky RL, Venkatakrishnan K. Mechanism-based inactivation of human cytochrome p450 enzymes and the prediction of drug-drug interactions. *Drug Metab Dispos*. 2007;35:246-255.
36. Yang J, Liao M, Shou M, et al. Cytochrome p450 turnover: regulation of synthesis and degradation, methods for determining rates, and implications for the prediction of drug interactions. *Curr Drug Metab*. 2008;9:384-394.
37. Boddy AV, Cole M, Pearson AD, Idle JR. The kinetics of the auto-induction of ifosfamide metabolism during continuous infusion. *Cancer Chemother Pharmacol*. 1995;36:53-60.
38. von Bahr C, Steiner E, Koike Y, Gabrielsson J. Time course of enzyme induction in humans: Effect of pentobarbital on nortriptyline metabolism*. *Clin Pharmac Therap*. 1998;64:18-26.
39. Mager DE, Wyska E, Jusko WJ. Diversity of mechanism-based pharmacodynamic models. *Drug Metab Dispos*. 2003;31:510-518.
40. Gamelin E, Boisdron-Celle M, Guérin-Meyer V, et al. Correlation between uracil and dihydrouracil plasma ratio, fluorouracil (5-FU) pharmacokinetic parameters, and tolerance in patients with advanced colorectal cancer: a potential interest for predicting 5-FU toxicity and determining optimal 5-FU dosage. *J Clin Oncol*. 1999;17:1105.
41. Jiang H, Lu J, Ji J. Circadian rhythm of dihydrouracil/uracil ratios in biological fluids: a potential biomarker for dihydropyrimidine dehydrogenase levels. *Br J Pharmacol*. 2004;141:616-623.
42. Sharma A, Ebling WF, Jusko WJ. Precursor-dependent indirect pharmacodynamic response model for tolerance and rebound phenomena. *J Pharm Sci*. 1998;87:1577-1584.
43. Meulendijks D, Henricks LM, Jacobs BAW, et al. Pretreatment serum uracil concentration as a predictor of severe and fatal fluoropyrimidine-associated toxicity. *Br J Cancer*. 2017;116:1415-1424.
44. Henricks LM, Jacobs BAW, Meulendijks D, et al. Food-effect study on uracil and dihydrouracil plasma levels as marker for dihydropyrimidine dehydrogenase activity in human volunteers. *Br J Clin Pharmacol*. 2018;84:2761-2769.
45. Ogura K, Ohnuma T, Minamide Y, et al. Dihydropyrimidine dehydrogenase activity in 150 healthy Japanese volunteers and identification of novel mutations. *Clin Cancer Res*. 2005;11:5104-5111.
46. Yamamoto N, Hayashi H, Planchard D, et al. A randomized, phase 2 study of deoxyuridine triphosphatase inhibitor, TAS-114, in combination with S-1 versus S-1 alone in patients with advanced non-small-cell lung cancer. *Invest New Drugs*. 2020;38:1588-1597.
47. Kawazoe A, Takahari D, Keisho C, et al. A multicenter phase II study of TAS-114 in combination with S-1 in patients with pretreated advanced gastric cancer (EPOC1604). *Gastric Cancer*. 2021;24:190-196.
48. Yokogawa T, Yano W, Tsukioka S, et al. dUTPase inhibition confers susceptibility to a thymidylate synthase inhibitor in DNA-repair-defective human cancer cells. *Cancer Sci*. 2021;112:422-432.

SUPPORTING INFORMATION

Additional supporting information may be found in the online version of the article at the publisher's website.

How to cite this article: Araki H, Takenaka T, Takahashi K, et al. A semimechanistic population pharmacokinetic and pharmacodynamic model incorporating autoinduction for the dose justification of TAS-114. *CPT Pharmacometrics Syst Pharmacol*. 2022;11:604-615. doi:10.1002/psp4.12747